Hypoxia inducible microRNA 210 attenuates keratinocyte proliferation and impairs closure in a murine model of ischemic wounds

Sabyasachi Biswas[a], Sashwati Roy[a], Jaideep Banerjee[a], Syed-Rehan A. Hussain[a], Savita Khanna[a], Guruguhan Meenakshisundaram[b], Periannan Kuppusamy[b], Avner Friedman[c,1], and Chandan K. Sen[a,1]

Departments of [a]Surgery and [b]Internal Medicine, Ohio State University Medical Center, Columbus, OH 43210; and [c]Mathematical Biosciences Institute, Ohio State University, Columbus, OH 43210

Contributed by Avner Friedman, February 16, 2010 (sent for review December 10, 2009)

Ischemia complicates wound closure. Here, we are unique in presenting a murine ischemic wound model that is based on bipedicle flap approach. Using this model of ischemic wounds we have sought to elucidate how microRNAs may be implicated in limiting wound re-epithelialization under hypoxia, a major component of ischemia. Ischemia, evaluated by laser Doppler as well as hyperspectral imaging, limited blood flow and lowered tissue oxygen saturation. EPR oximetry demonstrated that the ischemic wound tissue had pO_2 <10 mm Hg. Ischemic wounds suffered from compromised macrophage recruitment and delayed wound epithelialization. Specifically, epithelial proliferation, as determined by Ki67 staining, was compromised. In vivo imaging showed massive hypoxia inducible factor-1α (HIF-1α) stabilization in ischemic wounds, where HIF-1α induced miR-210 expression that, in turn, silenced its target E2F3, which was markedly down-regulated in the wound-edge tissue of ischemic wounds. E2F3 was recognized as a key facilitator of cell proliferation. In keratinocytes, knock-down of E2F3 limited cell proliferation. Forced stabilization of HIF-1α using Ad-VP16- HIF-1α under normoxic conditions up-regulated miR-210 expression, down-regulated E2F3, and limited cell proliferation. Studies using cellular delivery of miR-210 antagomir and mimic demonstrated a key role of miR-210 in limiting keratinocyte proliferation. In summary, these results are unique in presenting evidence demonstrating that the hypoxia component of ischemia may limit wound re-epithelialization by stabilizing HIF-1α, which induces miR-210 expression, resulting in the down-regulation of the cell-cycle regulatory protein E2F3.

skin | tissue repair | wound healing

In the United States, chronic wounds affect 6.5 million patients. An estimated excess of US$25 billion is spent annually on treatment of chronic wounds and the burden is rapidly growing because of increasing healthcare costs, an aging population, and a sharp rise in the incidence of diabetes and obesity worldwide (1). Ischemia is recognized as a factor that complicates wound healing. Vascular complications commonly associated with problematic wounds are primarily responsible for wound ischemia. Ischemia limits the supply of blood-borne products, including nutrients, oxygen, and circulating cells to the wound site, thereby severely impairing the healing response (2, 3). Animal wound healing models are important biological tools to understand basic processes of tissue repair and to develop and validate strategies for clinical treatment. Recently we have reported a preclinical large-animal model of ischemic wounds using a bipedicle flap approach (4). Although such a model is of high translational significance, enabling examination of clinically relevant problems, such models do not lend themselves to detailed scrutiny of molecular mechanisms because of limited availability of genetically modified animals, antibodies, and other molecular reagents. In this work, we are unique in presenting a report of a murine ischemic-wound model that is based on the approach of our large-animal model. Ischemia limits the supply of blood-borne products to the wound site, including oxygen. Thus, hypoxia is an integral component of ischemia (2). Using the recently developed murine model we have sought to elucidate how microRNAs may be implicated in limiting wound re-epithelialization under hypoxic conditions.

Results

Survival of skin flaps is known to depend on their dimension, which in turn determines the graded levels of ischemia throughout the flap tissue (5, 6). We chose to force skin ischemia by adopting a full-thickness bipedicle-flap approach that we have recently described in swine (4). The goal was to generate an ischemic piece of skin tissue that would survive for at least 2 weeks. First, we focused on optimizing the dimensions of the flap. Our efforts to identify the appropriate dimensions of the flap led to the observation that for bipedicle flaps, the length/breadth ratio of 3:1 that we had optimized in swine (4) was applicable to mice. We selected 30 mm length and 10 mm breadth as the final dimension (Fig. S1*A*).

Characterization of the state of tissue ischemia was performed by applying laser Doppler imaging (Fig. S1 *B* and *C*) and hyperspectral scanning (Fig. S2). Laser Doppler imaging is a useful technique for measuring microvascular perfusion in wounds because it involves no contact and produces a color image representing flow distribution over an area of tissue (7). Images shown in Fig. S1*B* demonstrate a clear contrast in blood flow between the flap and adjacent intact skin. The flaps were markedly ischemic compared to the intact skin (Fig. S1*C*). Hyperspectral scanning technology has recently emerged as being productive in characterizing tissue ischemia by noninvasively monitoring the tissue oxyhemoglobin and deoxyhemoglobin ratio (8). This technology has enabled the detection of early changes in the skin microcirculation in patients (9). The hypoxia component of tissue ischemia was characterized by hyperspectral scanning (Fig. S2). Compared with the intact skin, the flaps clearly suffered from hypoxic challenge. Quantitative analyses of the images demonstrated that the tissue-oxygen saturation at the ischemic wound site was half of the values collected from the adjacent intact skin (Fig. S2*B*). Direct measurement of tissue-oxygen tension using EPR oximetry provided consistent results (Fig. S3*B*). In vivo EPR spectra (Fig. S3*A*) were obtained using a LiNcBuO probe implanted in mouse skin (Fig. S3*C*). The peak-to-peak line widths were used to calculate pO_2 using a calibration curve. The oxygen tension at the ischemic wound site closely matched the values reported from ischemic wounds in patients. Clinically, in non-diabetics, chronic wounds are known to result when the wound-site pO_2 value is lower than 10 mm Hg (10–12). Consistently, in our

Author contributions: S.B., S.R., S.K., A.F., and C.K.S. designed research; S.B., S.R., J.B., S.-R.A.H., S.K., G.M., P.K., and C.K.S. performed research; S.B., S.R., J.B., S.-R.A.H., S.K., G.M., P.K., A.F., and C.K.S. analyzed data; and S.B., S.R., J.B., S.-R.A.H., S.K., G.M., P.K., A.F., and C.K.S. wrote the paper.

The authors declare no conflict of interest.

[1]To whom correspondence may be addressed. E-mail: chandan.sen@osumc.edu or friedman.158@osu.edu.

This article contains supporting information online at www.pnas.org/cgi/content/full/1001653107/DCSupplemental.

model we noted that the closure of ischemic wounds with pO_2 <10 mm Hg were significantly impaired (Fig. 1 *A* and *B*). Pair-matched histological characterization of the wound healing biology resulted in the observation that ischemic wounds suffered from impaired re-epithelialization (Fig. 1 *C* and *D*). Infiltration of macrophages into the wound site represents a key component of the acute inflammatory phase of wound healing (13). With the goal to study the inflammatory response to wounding, macrophages in the tissue sections were detected on day-3 wound sections using the pan-macrophage marker F4/80. Macrophage infiltration response was clearly blunted in pair-matched ischemic wounds (Fig. 1 *E* and *F*).

Wound-edge tissue were stained for keratin-14, the type I cytokeratin that forms the cytoskeleton of epithelial cells. Although the nonischemic healing wound showed clear presence of hyperproliferative epithelium (Fig. 2*A*), development of a hyperproliferative epithelium was severely compromised in the pair-matched ischemic wounds (Fig. 2*A*). Keratinocyte proliferation and migration represents two major events underlying wound re-epithelialization. Ki67$^+$ cells were noted in the basal region of the epithelium. Efforts to understand the mechanisms by which re-epithelialization is compromised in ischemic wounds led to the observation that in ischemic wounds epithelial cell proliferation is compromised (Fig. 2*B*). Hypoxia inducible factor-1α (HIF-1α) is a transcription factor that is known to regulate the hypoxic cell cycle. Recently, it has been demonstrated that in murine keratinocytes HIF-1α may arrest cell proliferation (14). Because HIF-1α is inducible by hypoxia, a component of ischemia (Figs. S1 and S2), the transactivation of HIF-1α was investigated in an in vivo wound setting using a bioluminescent imaging approach. HIF-1α transactivation was markedly stronger in ischemic wounds. The pair-matched difference between nonischemic and corresponding ischemic wounds was most prominent on day 3 postwounding (Fig. 3). HIF-1α is known to drive the expression of numerous coding genes. Recent works demonstrate that HIF-1α may also serve as a transcription factor for the expression of noncoding genes, including microRNAs (miRs) (15). miRs are now known to play a key role in cell proliferation (16). We observed that ischemic wounds have a higher abundance of the HIF-1α-dependent miR-210 (Fig. 4*A*). Of interest, expression of E2F3, which is a known target of miR-210 (17), was significantly lower in ischemic wounds (Fig. 4 *B* and *C*). Immunohistochemical studies identified abundant E2F3 in the epidermis of nonischemic wound (Fig. 4*D*). E2F3 in the wound-edge tissue of ischemic wounds was markedly down-regulated (Fig. 4*E*). These observations point toward a HIF-1α-driven miR210-dependent lowering of the cell proliferation mediator E2F3 in the wound-edge tissue.

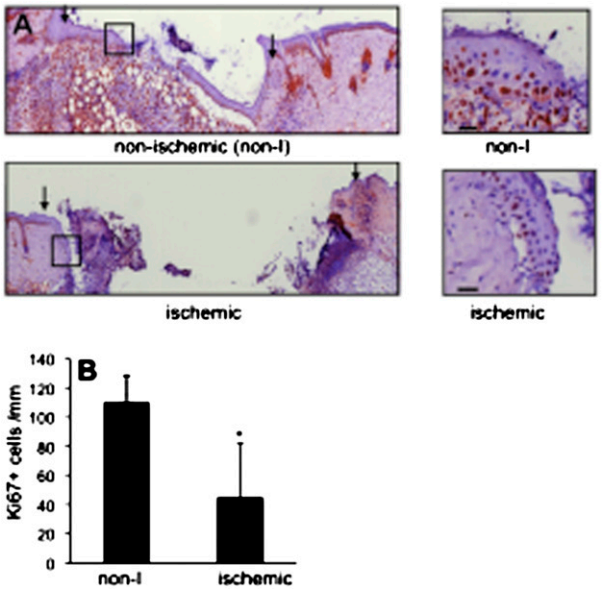

Fig. 2. Compromised epidermal cell proliferation (Ki67$^+$) in ischemic wounds. (*A*) Ki67 immunostaining (brown) was performed in day 3 wound sections. (*Left*) Mosaic-stitched image of wound sections; arrows indicate wound margin. (*Right*) Magnified epithelial tip region shown in corresponding right boxed area. (Scale bar, 50 μm.) (*B*) Quantification of Ki67$^+$ cells in epithelial tip region was measured and expressed as number per 1,000 μm length. Data are mean ± SD; n = 3. *, $P < 0.05$.

To test the significance of HIF-1α in regulating E2F3 and cell proliferation in keratinocytes, studies were performed using human HaCaT keratinocytes commonly used for the study of wound healing (18). Forced stabilization of HIF-1α in keratinocytes using Ad-VP16-HIF-1α under normoxic conditions provided an approach to specifically study the significance of HIF-1α. HIF-1α stabilization, adopting such genetic approach, resulted in attenu-

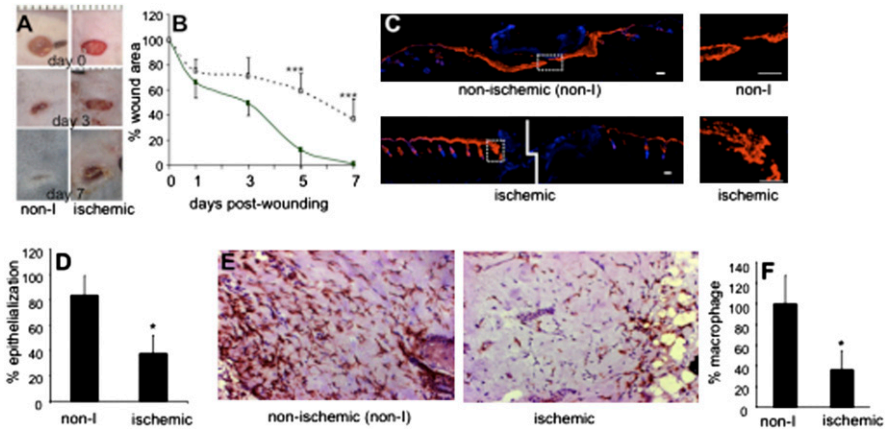

Fig. 1. Impaired healing in ischemic wounds. (*A*) Representative digital images of normoxic and ischemic wounds on days 0, 3, and 7 postwounding. (*B*) Closure of ischemic wounds. Data are presented as percent-wound area of initial wound size. Mean ± SD; n = 8; *, $P < 0.05$; and ***, $P < 0.001$ compared with nonischemic wounds. (*C*) Keratin 14 immunostaining (red) of day-3 wounds shows epithelialization. The sections were counterstained using DAPI (blue, nuclei). (Large images, *Left*) Stitched mosaic images showing the entire wound section; (small images, *Right*) magnified epithelial tip region shown in corresponding left panels with dotted box. (Scale bar, 50 μm.) (*D*) Wound epithelialization was quantified and expressed as percent-epithelialization. (*E*) Immunostaining for macrophages (brown) was performed on day-3 wound sections using the pan-macrophage marker F4/80 (Magnification, ×200). Sections were counterstained using hematoxylin (blue). (*F*) Macrophage infiltration was quantified using a color subtractive image processing tool. Data shown are mean ± SD; n = 5; *, $P < 0.05$.

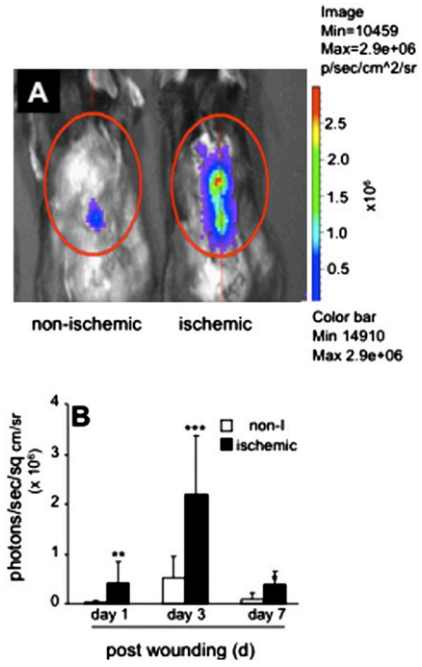

Fig. 3. Imaging of HIF-1α stabilization in ischemic wounds. (*A*) Representative in Vivo imaging system luminescent images of nonischemic or ischemic wounds showing hypoxia response element-luciferase reporter activity. Hypoxia response element-driven luciferase activation was imaged as a measure of HIF-1α stabilization in wounds. Repeated measurements from same mice on days 1, 3, and 7 postwounding were performed. (*B*) Quantitative measurement of luminescence in nonischemic and ischemic wounds. Open bar, nonischemic (non-I); solid bar, ischemic. Data are mean ± SD; $n = 3$ for each group; *, $P < 0.05$; **, $P < 0.01$; and ***, $P < 0.005$ compared with nonischemic wounds.

ated expression of E2F3 (Fig. 5 *A* and *B*), an observation that was consistent with the results from in vivo studies, suggesting that HIF-1α down-regulates E2F3 via a miR-210-dependent pathway. Knockdown of E2F3 limited cell proliferation, demonstrating the significance of E2F3 in driving the keratinocyte cell cycle. To examine whether HIF-1α stabilization is implicated in driving ischemia-inducible miR210 expression, Ad-VP16-HIF-1α was delivered to HaCaT keratinocytes under normoxic conditions to force stabilization of HIF-1α. HIF-1α stabilization in HaCaT under normoxic conditions resulted in marked induction of miR-210 expression, demonstrating that in keratinocytes miR-210 transcription is driven by HIF-1α (Fig. 6*A*). Using miR-210 antagomir and mimic, we were able to respectively down-regulate (Fig. 6*B*) and up-regulate (Fig. 6*C*) miR-210 expression in these keratinocytes. Down-regulation of basal miR-210 levels in keratinocytes significantly increased cell proliferation (Fig. 6*D*). Consistently, delivery of miR-210 mimic clearly compromised keratinocyte proliferation (Fig. 6*E*). Taken together these data show that, in keratinocytes, HIF-1α drives miR-210 expression, which in turn compromises cell proliferation by targeting E2F3. In summary, these results are unique in presenting evidence demonstrating that the hypoxia component of ischemia may limit wound re-epithelialization by stabilizing HIF-1α, which induces miR-210 expression, resulting in the down-regulation of the cell-cycle regulatory protein E2F3.

Discussion

Ischemic wounds are known to be associated with great loss of both limb and life (19, 20). Thus, clinically presented ischemic wounds do not readily lend themselves to the study of biological mechanisms because the collection of tissue biopsies at multiple timepoints from the same wound poses ethical challenges. The need for experimental models of ischemic wounds is therefore compelling. Skin flaps represent a proven classical approach to induce ischemia (5, 6, 21–23). In this study, the flap dimensions were optimized such that the tissue was ischemic but not necrotic. Such an approach enabled the pair-matched long-term study of a full-thickness wound placed at the most ischemic site of the skin tissue, compared with a similar wound placed on the adjacent perfused skin of the same animal. Ischemia is defined by lowered blood supply to the tissue and therefore compromised microcirculation. Limitations in the ability of the vasculature to deliver O_2-rich

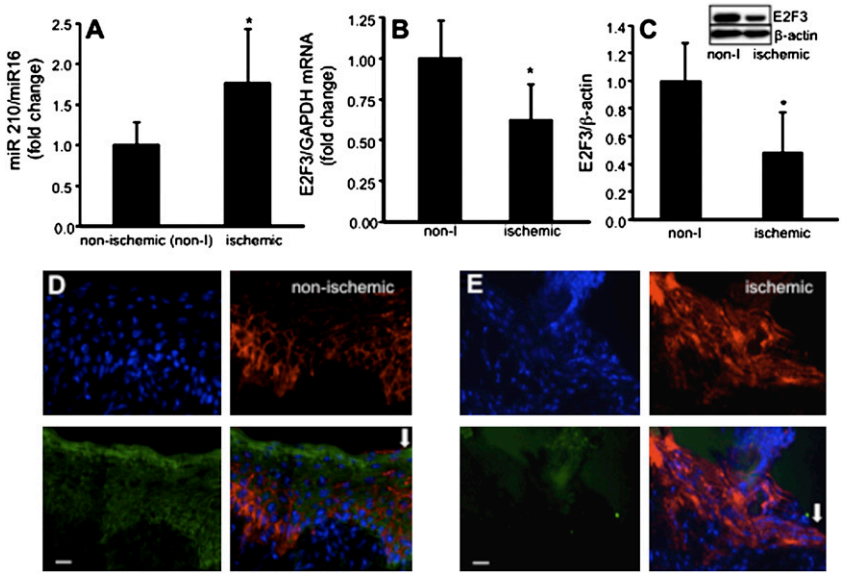

Fig. 4. Induction of miR-210 and down-regulation of E2F3 expression in ischemic wounds. (*A*) miR-210 expression in day 3 wound-edge tissue. miR-16 was used as housekeeping gene. Data are mean ± SD $n = 3$; *, $P < 0.05$. (*B*) E2F3 mRNA expression and (*C*) E2F3 protein expression (Western blot) in day 3 wound-edge tissues. Data are mean ± SD; $n = 3$; *, $P < 0.05$. (*D* and *E*) Immunostaining for E2F3 (green) and keratin 14 (red) was done on day-3 tissue sections from nonischemic (*D*) and ischemic (*E*) wounds. (*Upper Left*) Nuclear DAPI (blue stain); (*Upper Right*) K14 (red); (*Lower Left*) E2F3 (green); (*Lower Right*) overlay of all blue green and red demonstrating low expression of E2F3 in epidermal tissue of ischemic wounds. Arrow indicates wound edge. (Scale bar, 20 μm.)

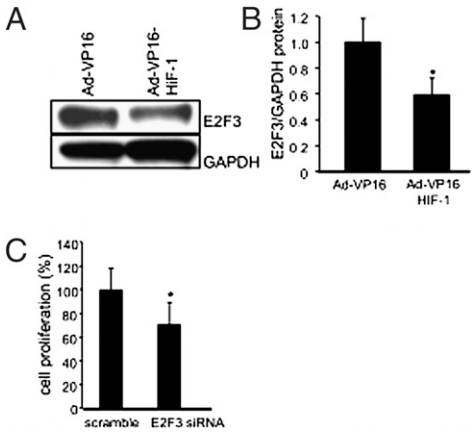

Fig. 5. E2F3 expression in human keratinocytes, a facilitator of cell proliferation, is down-regulated by forced stabilization of Hif-1α under normoxic conditions. (*A*) E2F3 expression was down-regulated in cells infected with Ad-VP16-HIF-1α compared with those infected with AdVP16 (control). A representative Western blot is shown. (*B*) Quantification of protein levels in *A* was performed by densitometry and data were normalized to GAPDH. Mean ± SD are shown; $n = 3$; *, $P < 0.05$. (*C*) Knock-down of E2F3 expression attenuated cell proliferation. Data are mean ± SD; $n = 6$; *, $P < 0.05$.

blood to the wound tissue leads to, among other consequences, hypoxia. Tissue hypoxia reflects a reduction in oxygen delivery below tissue demand, whereas ischemia is a lack of perfusion, characterized not only by hypoxia but also by insufficient supply of other blood-borne products including nutrients (2). In this study, the ischemic wounds had significantly lower blood flow as measured by laser Doppler imaging. Consistently, the ischemic wounds were hypoxic. Adult cutaneous tissue repair is accompanied by a robust recruitment of inflammatory cells to the wound site (13).

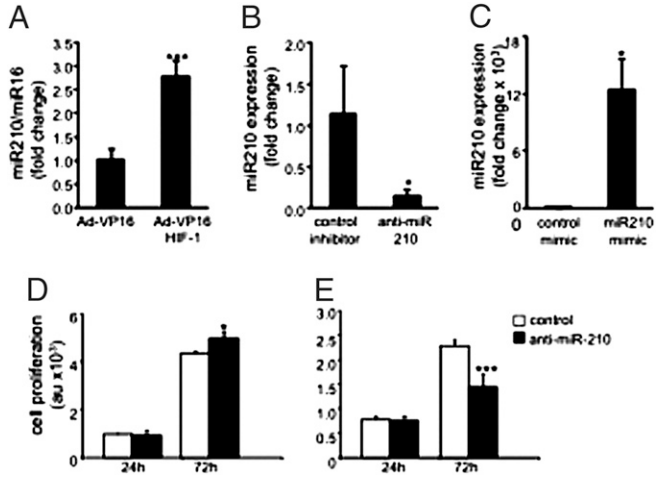

Fig. 6. Forced stabilization of Hif-1α under normoxic condition induced miR-210 expression and limited proliferation of human keratinocytes. (*A*) HaCaT cells were infected with AdVP16 (control) or AdVP16-HIF-1α viral vectors for 72 h. There was significant increase in miR-210 expression in HIF-1α-stabilized cells (Ad-VP16-HIF-1α viral infected group). Data shown as mean ± SD; $n = 3$; ***, $P < 0.001$. (*B*) Cells transfected with hsa-miR-210 stem-loop inhibitor (antagomir) shows a significant down-regulation of miR-210. (*C*) Transfection of cells with miR-210 mimic up-regulated cellular miR-210 abundance. Data are mean ± SD; $n = 4$; *, $P < 0.05$. (*D*) miR-210 down-regulation (as in *B*) increased cell proliferation. Control inhibitor, open bars; anti-miR-210, solid bars. Data are mean ± SD, $n = 3$. *, $P < 0.05$. (*E*) miR-210 up-regulation (as in *C*) compromised cell proliferation. Control mimic, open bars; miR-210 mimic, solid bars. Data are mean ± SD, $n = 3$; ***, $P < 0.0002$.

Timely recruitment of macrophages is necessary for wound healing (24, 25). In the nonischemic wounds, macrophage recruitment was markedly compromised, consistent with our observation in the preclinical setting (4).

Wound closure is the single-most important outcome, as viewed by the United States Food and Drug Administration, when evaluating wound-related therapeutics (26). Keratinocyte migration and proliferation both play a role in covering skin wounds by the process of re-epithelialization. Defects in this function are associated with the clinical phenotype of chronic nonhealing wounds. Ischemia is known to limit re-epithelialization (27–29). In the present study, ischemic wounds suffered from impaired re-epithelialization. Consistent with previous observations, ischemic conditions clearly compromised the formation of hyperproliferative epithelium (4). E2F transcription factors are central to epidermal morphogenesis and regeneration after injury (30). E2F DNA binding is known to be associated with keratinocyte proliferation (31). Chromatin immunoprecipitation analysis demonstrated that the cyclin A promoter is predominantly bound in proliferating keratinocytes by complexes containing E2F3 and that E2F3 is implicated in epidermal formation (32). E2F3, a known target of miR-210 (17), emerges as an important mediator of hypoxia-induced impairment of re-epithelialization of the ischemic wound.

HIF-1α has been widely known as a transcription factor that regulates the expression of several coding genes. miR-210 has recently emerged as a key noncoding gene that is transcriptionally driven by HIF-1α, adding a previously unexplored dimension to HIF-1α's circle of influence in molecular and cell biology. So far, the connection between HIF-1α and miR-210 has been studied in the context of cancer (17, 33). This work links miR-210 as a key regulator of ischemic wound closure. Recent work demonstrates that miR-210 may repress mitochondrial respiration and associated downstream functions (34). This association could be of importance in the healing wound, where metabolic demand on mitochondrial metabolism is known to be high. Thus, miR-210-directed therapeutic strategies to address complications in ischemic wound closure may prove to be a prudent consideration.

Materials and Methods

Animals. Commercially available C57BL/6 mice, obtained from Harlan Laboratories Inc., were used for the experiments. Adult (8-week-old mice, ~25 g in weight) were used for experiments. All studies were performed in compliance with the Institutional Animal Care and Use Committee of Ohio State University. Mice were housed individually after wounding with a 12-h light/dark cycle and temperature in the institutional animal facilities, and allowed access to food and water ad libitum, as described previously (13).

Wounding and Planimetry. Mice were anesthetized with an i.p. injection of ketamine (75 mg/kg) and xylazine (5 mg/kg) and then maintained under isoflurane. The dorsum was shaved, cleaned, and sterilized. A bipedicle flap was developed on the back of the mice by making 30-mm-long full-thickness parallel incisions 10 mm apart (Fig. S1*A*). Flap edges were cauterized and then sutured to the adjacent skin. Full-thickness excisional wounds were developed in the middle of each flap with a 3-mm disposable biopsy punch. Two more wounds (control nonischemic) were developed similarly in nonischemic skin at the same cranio-caudal location. Digital images of the wounds were taken on the days as indicated. Wound area measurement was done by digital planimetry using Image-J software (NIH), as described previously (4, 35).

Laser Doppler Measurements. The MoorLDI-Mark 2 laser Doppler blood-perfusion imager (Moor Instruments Ltd.) was used to map tissue blood flow, as described previously (4, 36).

Hyperspectral Imaging. Hyperspectral imaging was performed using OxyVu-2 system (Hypermed Inc.) according to the manufacturer's instructions, as reported previously (4).

EPR Oximetry. EPR oxymetry was performed as described previously (37). Oxygen-sensing probe octa-n-butoxynaphthalocyanine (LiNc-BuO) particles were implanted in each animal at two locations: in the center of the flap and

outside the flap (control), along the same craniocaudal plane. Anesthesia was administered using isoflurane, delivered with room air, during the surgical procedure and EPR measurements. EPR measurements were performed using an L-band (1.2 GHz) spectrometer (Magnettech) and a surface-loop resonator. The peak-to-peak line widths, obtained from EPR spectra, were used to calculate pO_2 using a calibration curve.

In Vivo Imaging System. HIF-1α transactivation was measured using a HIF-1α response element-luciferase (HRE-Luc) promoter-reporter construct (38). Ischemic flaps were developed as described above. Each wound was injected intracutaneously with 5×10^9 pfu Ad-HRE/LUC. For imaging, the substrate luciferin (Caliper Life Sciences), in 0.9% saline, was injected into the i.p. cavity at a dose of 150 mg/kg body weight and images were collected using an in vivo imaging system Series 100 (Xenogen) equipment after 20 min, with an integration time of 1 min. Overlay images and luminescent measurements were made using Living Image software (Version 2.50.1, Xenogen), as described previously (38).

Immunohistochemistry. Immunostaining for macrophages was performed on 10-μm thick cryosections of day-3 wounds using the pan-macrophage marker F4/80 (AbD Serotec). Quantitation was performed using a color subtractive technique, as described previously (4, 39). Epithelial tissue was visualized by immunostaining 10-μm thick cryosections of day-3 wounds for Keratin 14 (Covance) from the center of the wound. Fluorescent images were obtained after incubating with Alexa488 conjugated secondary antibody and counterstaining with DAPI. The cell proliferation marker Ki67 (Dako Cytomation) was used to immunostain day-3 cryosections. Positively stained cells are seen in the basal region of the epithelium. $Ki67^+$ cells were enumerated along the length of the wound-edge epithelium and expressed as number of positive cells per millimeter of the wound-edge epithelium. Positive cells were counted using the "Measure Events" function of the Axiovision V4.6 software (Carl Zeiss Microimaging).

Western Blot. Western blot was performed as described previously (4, 13, 40). Primary antibodies against E2F3 (dilution 1:4,000, Lifespan Biosciences), β-actin (dilution 1:5,000, Sigma-Aldrich), and GAPDH (dilution 1:10,000) were used to detect these antigens.

Hif-1α Stabilization in Human Keratinocytes. Adenoviruses expressing a plasmid encoding a fusion protein of amino acids 1 to 529 of HIF-1α and the herpes simplex virus VP16 transactivation domain (pBABE-puro-HIF-1α-VP16) and a control plasmid encoding only VP16 (pBABE-puro-VP16) were used for transfecting the cells (41). HaCaT cells were grown in standard 12-well plates to 75% confluence. Next, cells were transfected with 2.3×10^9 pfu Ad-VP16-HIF-1α or with the empty vector as control in 750 μL of media. Subsequently, 750 μL of additional media was added 4 h later and the cells were incubated for 72 h.

Cell Culture. Human immortalized keratinocytes (HaCaT) were grown under standard culture conditions (at 37 °C in a humidified atmosphere consisting of 95% air and 5% CO_2) in DMEM growth medium supplemented with 10% FBS, 100 IU/mL penicillin, 0.1 mg/mL streptomycin, and 10 mmol/L L-glutamine (GIBCO-BRL) as described previously (18).

siRNA/miRNA Delivery to Cells. Transfection of HaCaT cells was performed as described (42). Briefly, HaCaT cells (0.2×10^6 cells per well in 12-well plate) were seeded in antibiotic-free DMEM medium 24 h before transfection. DharmaFECT 1 transfection reagent (Dharmacon RNA Technologies) was used to transfect cells with 100 nmol/L siRNA smart pool, for human E2F3, or hsa-miR210 stem-loop inhibitor and hsa-miR-210 mimic (Dharmacon Technologies). Transfection of nontargeting siRNA/or miRNA inhibitor negative controls was performed for the control groups. Cells were harvested after 72 h of such treatments.

Quantification of mRNA and miRNA Expression Levels. Total RNA, including the miRNA fraction, was isolated using *mir*Vana miRNA isolation kit, according to the manufacturer's protocol (Ambion Inc.). Specific Taqman assays for miRNA (Applied Biosystems) and *mir*Vana qRT-PCR miRNA RT Kit (Applied Biosystems) were used with real-time PCR system and Taqman universal master mix. Levels of miRNA were quantified with the relative quantification method using either snoRNA or miR-16 as the housekeeping miRNA. The transcription levels of E2F3 and house keeping control β-actin was quantified using SYBR green-I (Applied Biosystems). Expression levels of miRNA and mRNA were quantified employing the 2 (-ΔΔct) relative quantification method.

Cell Proliferation Assay. Transfected cells were reseeded in 96-well plates and assayed for cell proliferation using CyQUANT cell proliferation assay kit (Invitrogen) as previously described (42).

Statistics. Pair-matched ischemic and nonischemic wounds in the same mouse were compared by paired *t* test. Student's *t* test was used for all other comparison of difference between means. $P < 0.05$ was considered significant.

ACKNOWLEDGMENTS. This work was supported in part by National Institutes of Health Grants RO1 GM 077185 and GM 069589 (to C.K.S.) and RO1 DK076566 (to S.R.).

1. Sen CK, et al. (2009) Human skin wounds: a major and snowballing threat to public health and the economy. *Wound Repair Regen* 17:763–771.
2. Sen CK (2009) Wound healing essentials: let there be oxygen. *Wound Repair Regen* 17:1–18.
3. Powell RJ, et al. (2008) Results of a double-blind, placebo-controlled study to assess the safety of intramuscular injection of hepatocyte growth factor plasmid to improve limb perfusion in patients with critical limb ischemia. *Circulation* 118:58–65.
4. Roy S, et al. (2009) Characterization of a preclinical model of chronic ischemic wound. *Physiol Genomics* 37:211–224.
5. Kerrigan CL, Daniel RK (1984) Skin flap research: a candid view. *Ann Plast Surg* 13: 383–387.
6. Kerrigan CL, Daniel RK (1982) Critical ischemia time and the failing skin flap. *Plast Reconstr Surg* 69:986–989.
7. Khan F, Newton DJ (2003) Laser Doppler imaging in the investigation of lower limb wounds. *Int J Low Extrem Wounds* 2:74–86.
8. Khaodhiar L, et al. (2007) The use of medical hyperspectral technology to evaluate microcirculatory changes in diabetic foot ulcers and to predict clinical outcomes. *Diabetes Care* 30:903–910.
9. Greenman RL, et al. (2005) Early changes in the skin microcirculation and muscle metabolism of the diabetic foot. *Lancet* 366:1711–1717.
10. Mathieu D, Mani R (2007) A review of the clinical significance of tissue hypoxia measurements in lower extremity wound management. *Int J Low Extrem Wounds* 6: 273–283.
11. Franzeck UK, Talke P, Bernstein EF, Golbranson FL, Fronek A (1982) Transcutaneous PO2 measurements in health and peripheral arterial occlusive disease. *Surgery* 91: 156–163.
12. Harward TR, Volny J, Golbranson F, Bernstein EF, Fronek A (1985) Oxygen inhalation—induced transcutaneous PO2 changes as a predictor of amputation level. *J Vasc Surg* 2:220–227.
13. Roy S, Khanna S, Rink C, Biswas S, Sen CK (2008) Characterization of the acute temporal changes in excisional murine cutaneous wound inflammation by screening of the wound-edge transcriptome. *Physiol Genomics* 34:162–184.
14. Scortegagna M, Martin RJ, Kladney RD, Neumann RG, Arbeit JM (2009) Hypoxia-inducible factor-1alpha suppresses squamous carcinogenic progression and epithelial-mesenchymal transition. *Cancer Res* 69:2638–2646.
15. Sen CK, Gordillo GM, Khanna S, Roy S (2009) Micromanaging vascular biology: tiny microRNAs play big band. *J Vasc Res* 46:527–540.
16. Gammell P (2007) MicroRNAs: recently discovered key regulators of proliferation and apoptosis in animal cells : Identification of miRNAs regulating growth and survival. *Cytotechnology* 53:55–63.
17. Giannakakis A, et al. (2008) miR-210 links hypoxia with cell cycle regulation and is deleted in human epithelial ovarian cancer. *Cancer Biol Ther* 7:255–264.
18. Sen CK, et al. (2002) Oxidant-induced vascular endothelial growth factor expression in human keratinocytes and cutaneous wound healing. *J Biol Chem* 277:33284–33290.
19. Quirinia A (2000) Ischemic wound healing and possible treatments. *Drugs Today (Barc)* 36:41–53.
20. Slovut DP, Sullivan TM (2008) Critical limb ischemia: medical and surgical management. *Vasc Med* 13:281–291.
21. Fujihara Y, et al. (2008) Controlled delivery of bFGF to recipient bed enhances the vascularization and viability of an ischemic skin flap. *Wound Repair Regen* 16: 125–131.
22. Mittermayr R, et al. (2008) Sustained (rh)VEGF(165) release from a sprayed fibrin biomatrix induces angiogenesis, up-regulation of endogenous VEGF-R2, and reduces ischemic flap necrosis. *Wound Repair Regen* 16:542–550.
23. Tanaka R, et al. (2008) The effects of flap ischemia on normal and diabetic progenitor cell function. *Plast Reconstr Surg* 121:1929–1942.
24. Leor J, et al. (2006) Ex vivo activated human macrophages improve healing, remodeling, and function of the infarcted heart. *Circulation* 114 (1, Suppl):I94–I100.
25. Orenstein A, et al. (2005) Treatment of deep sternal wound infections post-open heart surgery by application of activated macrophage suspension. *Wound Repair Regen* 13:237–242.
26. Food and Drug Administration (2006), ed. Services, U.S.D.o.H.a.H. (Food and Drug Administration, Regulatory Guidance.) http://www.fda.gov/downloads/Drugs/GuidanceComplianceRegulatoryInformation/Guidances/ucm071324.pdf.

27. Kopal C, Deveci M, Oztürk S, Sengezer M (2007) Effects of topical glutathione treatment in rat ischemic wound model. *Ann Plast Surg* 58:449–455.
28. Liechty KW, et al. (1999) Adenoviral-mediated overexpression of platelet-derived growth factor-B corrects ischemic impaired wound healing. *J Invest Dermatol* 113: 375–383.
29. Sun W, et al. (2007) Collagen membranes loaded with collagen-binding human PDGF-BB accelerate wound healing in a rabbit dermal ischemic ulcer model. *Growth Factors* 25:309–318.
30. Chang WY, Andrews J, Carter DE, Dagnino L (2006) Differentiation and injury-repair signals modulate the interaction of E2F and pRB proteins with novel target genes in keratinocytes. *Cell Cycle* 5:1872–1879.
31. Jones SJ, Dicker AJ, Dahler AL, Saunders NA (1997) E2F as a regulator of keratinocyte proliferation: implications for skin tumor development. *J Invest Dermatol* 109: 187–193.
32. Chang WY, Bryce DM, D'Souza SJ, Dagnino L (2004) The DP-1 transcription factor is required for keratinocyte growth and epidermal stratification. *J Biol Chem* 279: 51343–51353.
33. Huang X, et al. (2009) Hypoxia-inducible mir-210 regulates normoxic gene expression involved in tumor initiation. *Mol Cell* 35:856–867.
34. Chan SY, et al. (2009) MicroRNA-210 controls mitochondrial metabolism during hypoxia by repressing the iron-sulfur cluster assembly proteins ISCU1/2. *Cell Metab* 10: 273–284.
35. Ojha N, et al. (2008) Assessment of wound-site redox environment and the significance of Rac2 in cutaneous healing. *Free Radic Biol Med* 44:682–691.
36. Roy S, Khanna S, Nallu K, Hunt TK, Sen CK (2006) Dermal wound healing is subject to redox control. *Mol Ther* 13:211–220.
37. Meenakshisundaram G, et al. (2009) Oxygen sensitivity and biocompatibility of an implantable paramagnetic probe for repeated measurements of tissue oxygenation. *Biomed Microdevices* 11:817–826.
38. Ratan RR, et al. (2008) Small molecule activation of adaptive gene expression: tilorone or its analogs are novel potent activators of hypoxia inducible factor-1 that provide prophylaxis against stroke and spinal cord injury. *Ann N Y Acad Sci* 1147:383–394.
39. Underwood RA, Gibran NS, Muffley LA, Usui ML, Olerud JE (2001) Color subtractive-computer-assisted image analysis for quantification of cutaneous nerves in a diabetic mouse model. *J Histochem Cytochem* 49:1285–1291.
40. Roy S, et al. (2007) Transcriptome-wide analysis of blood vessels laser captured from human skin and chronic wound-edge tissue. *Proc Natl Acad Sci USA* 104:14472–14477.
41. Aminova LR, et al. (2005) Prosurvival and prodeath effects of hypoxia-inducible factor-1alpha stabilization in a murine hippocampal cell line. *J Biol Chem* 280: 3996–4003.
42. Shilo S, Roy S, Khanna S, Sen CK (2008) Evidence for the involvement of miRNA in redox regulated angiogenic response of human microvascular endothelial cells. *Arterioscler Thromb Vasc Biol* 28:471–477.